

Invited Review

Dipolar and Scalar Couplings in Solid State NMR of Quadrupolar Nuclei

Alexej Jerschow*

Department of Chemistry, New York University, New York, NY 10003

Received April 16, 2002; accepted May 15, 2002

Published online October 7, 2002 © Springer-Verlag 2002

Summary. Most NMR-active nuclei found in the periodic table have a quadrupole moment. In combination with a nonsymmetric electron distribution a strong NMR-active interaction results, which very often overshadows the dipolar and scalar couplings. This article aims at reviewing how these interactions manifest themselves in quadrupolar NMR and how they can be exploited for resonance assignment and structure elucidation, in spite of the presence of a strong quadrupolar interaction.

Keywords. Solid-state; NMR spectroscopy; Dipolar couplings; Quadrupolar couplings.

Introduction

Most NMR-active nuclei in the periodic table have a quadrupole moment, that is a nonsymmetric nuclear charge distribution. In combination with a nonsymmetric electron distribution a strong NMR-active interaction results, which very often overshadows other interactions such as dipolar and scalar couplings. It is on the basis of observing and interpreting manifestations of these interactions that structure elucidation has been extremely successful in spin 1/2 NMR in one and multiple dimensions in both the liquid and the solid states [1, 2]. Dipolar couplings allow the determination of interatomic distances *via* NOESY-type experiments [1, 3] in the liquid state and dipolar recoupling techniques [4–6] and dipolar correlation experiments [7] in the solid state. Correlation spectroscopy *via* scalar *J* couplings is routinely applied in the liquid state (COSY-type experiments) and has likewise been demonstrated in solid state NMR [8–11] (see Ref. [12] for a recent comprehensive review).

In solid-state NMR of quadrupolar nuclei these approaches have not been as successful because the dipolar and scalar couplings are often negligible compared

* E-mail: alexej.jerschow@nyu.edu

to the dominant quadrupolar coupling. Notable exceptions are cases where the quadrupolar couplings are comparatively weak, such as *e.g.* in ${}^6\text{Li}$ and ${}^7\text{Li}$ NMR.

This article aims at reviewing how dipolar and scalar couplings manifest themselves in solid state quadrupolar NMR and how they can be exploited for resonance assignment and structure elucidation in cases where the quadrupolar coupling is large compared to these interactions.

One-dimensional NMR

Because of the strength of the quadrupolar coupling interaction, which may be on the order of several MHz, dipolar and scalar couplings have rarely been observed in static one-dimensional NMR experiments. The strength of the dipolar coupling interaction may be on the order of hundreds of Hz up to a kHz (*e.g.* 532 Hz for Mn–Mn with a distance of 2.4 Å), which is minute compared to the quadrupolar interaction (*e.g.* a linewidth of 2 MHz due to a typical quadrupolar coupling strength covers 100 times the full ${}^{13}\text{C}$ chemical shift range at a 100 MHz *Larmor* frequency). Heteronuclear dipolar coupling constants to protons may be as large as 10 kHz (*e.g.* 9.3 kHz for ${}^{27}\text{Al}$ – ${}^1\text{H}$ with a 1.5 Å distance), but are nonetheless significantly weaker than common quadrupolar couplings. Reports of observations of these couplings can therefore be expected to be scarce. For half-integer spins, where the central transition is free from the first order quadrupolar broadening [13] it should, however, be straightforward to observe dipolar as well as scalar couplings in an additional linebroadening and linesplitting of the central transition lines, since the second order quadrupolar broadening is on the order of just a few kHz. Figure 1 shows experimental and simulated static powder lineshapes for [${}^{17}\text{O}$] and [${}^{13}\text{C}$, ${}^{17}\text{O}$]benzamide. The former displays a usual second order powder lineshape expected for the central transition of a quadrupolar nucleus. The latter shows additional splitting resulting from the dipolar couplings between the ${}^{13}\text{C}$ and the ${}^{17}\text{O}$ nuclei. In this case these additional lineshape effects were used to determine the absolute orientations of the electric field gradient tensor components and the internuclear ${}^{13}\text{C}$ – ${}^{17}\text{O}$ vector.

First Order Effects

Magic angle spinning (MAS) has been employed successfully in NMR of spin 1/2 nuclei to obtain high resolution spectra. In quadrupolar NMR this method also leads to significant line narrowing due to (a) the removal of the first order quadrupolar coupling and (b) the reduction of the second order quadrupolar coupling (see below). One would think that here the dipolar couplings should be easy to observe, since one only needs to compete with the second order quadrupolar broadening (on the order of a few kHz). The dipolar couplings are, however, likewise averaged away rather efficiently by MAS. The strength and orientation parameters of the dipolar couplings can in theory (in theory only) be determined by analysing the intensities of the spinning sidebands [14]. The quadrupolar couplings also contribute to the intensities and due to the relative weakness of the dipolar couplings this approach seems prohibitive. It should be mentioned, however, that analysing the spinning sidebands in the spectra of spin 1/2 nuclei coupled to quadrupolar nuclei is

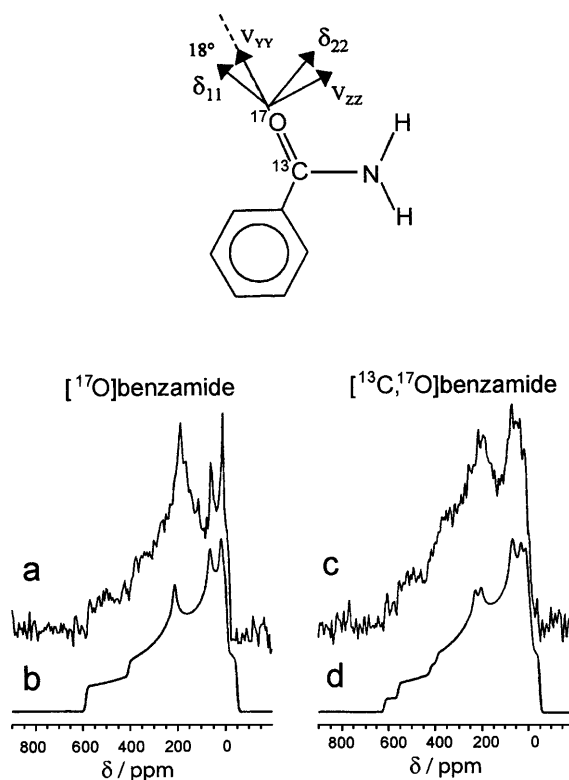


Fig. 1. Experimental and simulated static powder lineshapes for ^{17}O benzamide (a,b) and $^{13}\text{C}, ^{17}\text{O}$ benzamide (c, d). The additional linesplitting in (c) and (d) arises from the dipolar couplings between the ^{13}C and the ^{17}O nuclei (reproduced from Ref. [81], with permission)

a straightforward procedure that has provided useful structural information based on dipolar couplings [15–17].

Scalar coupling (the isotropic part), on the other hand should still be observable as it is independent of orientation. Its small strength (up to a few hundred Hz), however, makes its observation rather difficult. Figure 2 shows one of the few documented observations of scalar coupling in a spectrum of a quadrupolar nucleus [18]. While the coupling has a perceptible effect on the powder lineshape it should be noted that in this particular case the presence of the isotropic J coupling has been established by other means (see below). Again, scalar couplings between $1/2$ and quadrupolar nuclei are best observed in the spectrum of the spin $1/2$ nucleus [19].

Second Order Effects

It is well known that MAS NMR spectra of spin $1/2$ nuclei coupled to quadrupolar nuclei (*e.g.* ^{14}N) show peculiar non-symmetric lineshapes and linesplittings, which can be explained by a second order dipolar coupling (a cross-term between the quadrupolar and the dipolar coupling) [20, 21]. This additional linebroadening is not averaged away by MAS. It scales as $\omega_Q\omega_D/\omega_0$, where $\omega_Q = C_Q/2I(2I-1)$, with C_Q the nuclear quadrupolar coupling constant, ω_D the dipolar coupling constant,

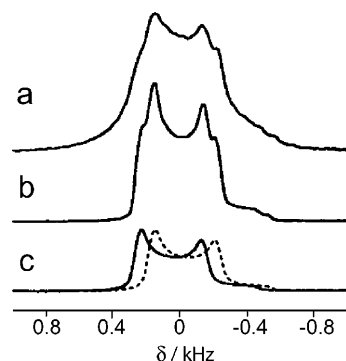


Fig. 2. ^{11}B MAS spectra of $(\text{PhO})_3\text{P-BH}_3$ obtained at 7.4 T. (a) Experimental spectrum, (b) simulated spectrum, and (c) simulated subspectra for the two components of the doublet arising from J coupling to ^{31}P . A coupling constant of approximately 85 Hz was extracted (reproduced from Ref. [18], with permission)

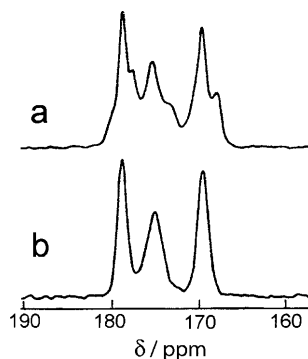


Fig. 3. ^{13}C MAS spectra showing (a) residual second order dipolar lineshape distortions arising from coupling to ^{14}N , and (b) their removal by isotopically enriching the molecule with ^{15}N . The spectra arise from the cyanide carbons of the coordination polymer $[(\text{Me}_3\text{Sn})_4\text{Fe}(\text{CN})_6]_\infty$. There are three cyanide environments in the crystal structure (reproduced from Ref. [21], with permission)

and ω_0 the *Larmor* frequency, given in angular velocity units. The resonance broadening and splitting effects can be on the order of up to a few hundred Hz. Figure 3 shows a ^{13}C MAS spectrum where the residual second order dipolar coupling to ^{14}N leads to pronounced lineshape distortions. The authenticity of the lineshape effects is tested by acquiring the same spectrum from an ^{15}N labeled sample, where the distortions disappear. Similar effects have been observed for many nuclear pairs, including ^{31}P - $^{63/65}\text{Cu}$, ^{31}P - ^{55}Mn , ^{119}Sn - $^{35/37}\text{Cl}$, ^{13}C - ^{23}Na , ^{29}Si - ^{14}N , and even ^{13}C - ^2H [21]. In the latter case the quadrupolar couplings are comparatively weak, but the larger dipolar couplings associated with the deuterium nucleus compensate for this [22].

In a MAS NMR spectrum of a quadrupolar nucleus, where the linewidth resulting from the second order quadrupolar coupling can be a few kHz in size, these effects are also expected to be visible. Likewise, homonuclear coupling between two quadrupolar nuclei should have pronounced effects. Because of the complicated orientational dependencies involved (the second order dipolar/quadrupolar

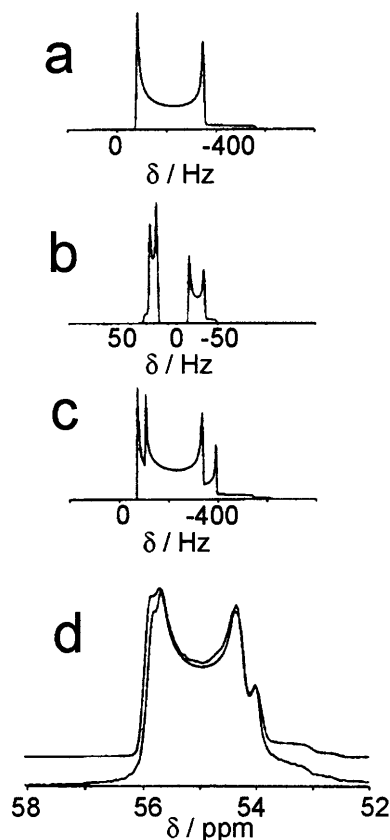


Fig. 4. Simulated central transition ^{11}B MAS NMR spectra arising from the second-order ^{11}B quadrupolar interaction (a), the residual second order ^{11}B - ^{14}N dipolar interaction alone (b), and both interactions (c). (d) Experimental ^{11}B MAS NMR spectrum of triethanolamine borate obtained at 11.75 T (adapted from Ref. [24], with permission)

cross-term depends on the strength and orientations of the quadrupolar tensor, as well as, on the orientation of the internuclear vector and the distance between the nuclei) additional lineshape effects, though sufficiently strong, may not be immediately apparent in a one-dimensional MAS spectrum of a powder sample (see for example Ref. [23]). Figure 4 shows simulations and experimental evidence of lineshape distortions of the central transition signal of ^{11}B [24] in the presence of a residual dipolar coupling to ^{14}N .

Dipolar Recoupling

The (first order) dipolar interaction is normally averaged out over a rotor cycle by MAS (see Fig. 5). However, if this time averaging is interrupted by the application of rotor-synchronized rf irradiation, a non-vanishing effective dipolar coupling arises (Fig. 5b) [4, 5]. Heteronuclear dipolar interactions have been recoupled in this way for spin 1/2 nuclei by a technique called REDOR (Rotational Echo Double Resonance), which uses two π pulses per rotor cycle [6]. Approximately 70% of the dipolar coupling can be recoupled using REDOR. This coupling leads

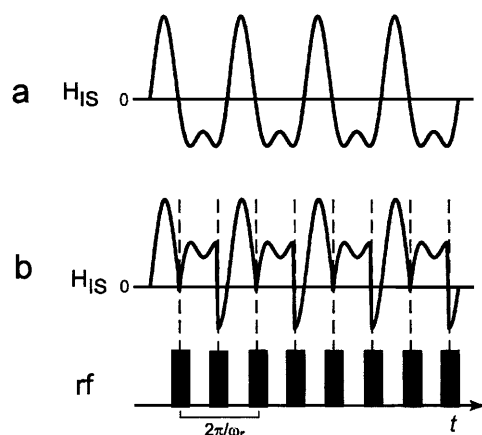


Fig. 5. The dipolar interaction is averaged away by MAS. (a) Shows an example of the change of the magnitude of the heteronuclear dipolar Hamiltonian during the rotation for a particular crystallite orientation. (b) Shows how the averaging process can be interrupted by the application of 180 degree pulses during the rotor period. An average dipolar interaction results

to a signal dephasing, which is recorded after different recoupling times. A “dephasing curve” is obtained which can be used to extract the dipolar coupling constants [6]. The pulse sequence of the REDOR experiment is shown in Fig. 6a.

This approach has also been successfully implemented for determining distances between quadrupolar and spin 1/2 nuclei, and even between different quadrupolar nuclei (*e.g.* ^{11}B and ^{27}Al) [25, 26]. In many cases, however, REDOR is not very efficient since it relies on the possibility of complete magnetization inversion for a quadrupolar nucleus. This is rarely possible. Another approach, called TRAPDOR (transfer of populations in double resonance), has been shown to give better sensitivity to dipolar couplings. In this case a continuous rf field is applied to the quadrupolar nucleus and several level transitions occur adiabatically over a rotor cycle (Fig. 6b shows the pulse sequence). While REDOR affects for the most part only the $\pm\frac{1}{2}$ states, TRAPDOR affects all levels and therefore leads to more effective dephasing [27–29]. In this way decay curves can be acquired, which are characteristic of the dipolar and quadrupolar couplings. While the extraction of quantitative information relies on computer simulations and is sometimes cumbersome, this technique has been very useful to detect nuclei with large quadrupolar couplings “indirectly”. This is done by monitoring the decay of the magnetization of a spin 1/2 nucleus coupled to the quadrupolar spin as a function of the offset of the rf field applied to the quadrupolar spin [30, 31]. Two spectra need to be acquired, one with rf irradiation at the *Larmor* frequency of the quadrupolar nucleus, and one without. The difference spectrum shows the spectrum of the nuclei coupled to the quadrupolar nucleus. An example is shown in Fig. 7, where the signals from the ^{31}P nuclei neighboring ^{27}Al nuclei were filtered out.

Sometimes the TRAPDOR experiment can become difficult to perform because of rf power and irradiation time limits. The REAPDOR experiment (Rotational echo, adiabatic passage, double resonance) can prove more useful in these cases. Instead of a continuous wave irradiation on the quadrupolar nucleus for a duration of several rotor cycles (up to several milliseconds) a spin-lock pulse is applied for

Couplings in Solid State NMR

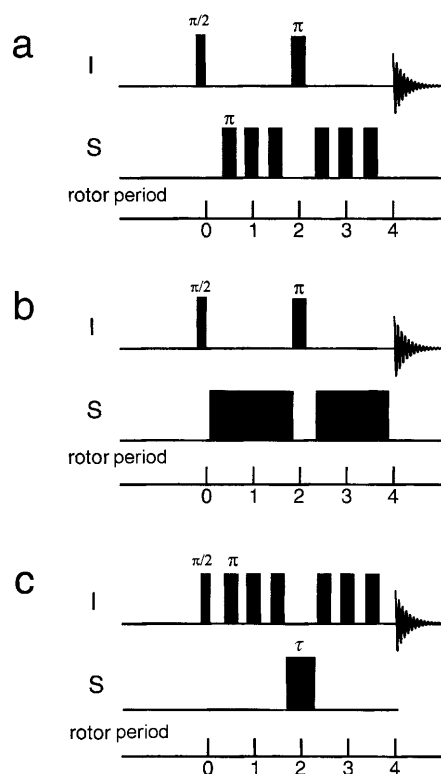


Fig. 6. (a) The REDOR pulse sequence. Two 180 degree pulses per rotor period recouple the dipolar coupling. (b) The TRAPDOR sequence. A continuous wave field applied to the quadrupolar nucleus (S) over several rotor periods recouples the dipolar coupling. (c) The REAPDOR sequence. The dipolar coupling is recoupled by two 180 degree pulses per rotor period on the spin 1/2 nucleus (I) and a continuous wave field on the quadrupolar nucleus (S) for approximately 1/3 of a rotor period

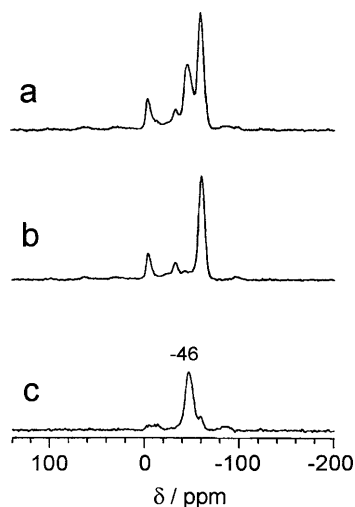


Fig. 7. $^{31}\text{P}/^{27}\text{Al}$ TRAPDOR experiment of trimethylphosphine on dehydroxylated zeolite HY. Without ^{27}Al irradiation (a), with irradiation (b), and the TRAPDOR spectrum (c) which is the difference between (a) and (b) (reproduced from Ref. [30], with permission)

only a fraction of a rotor period (Fig. 6c shows the pulse sequence). The rest of the time 180 degree pulses on the neighboring spin 1/2 nucleus prevent the dipolar coupling from refocusing. At the same time the effects of the chemical shift anisotropies are eliminated during the dephasing time. The spin-lock pulse on the quadrupolar nucleus partly inverts the populations of the quadrupolar nucleus. The optimal duration of the pulse needs to be adjusted individually but is approximately 1/3 of the rotor period. Without it the second half of the pulse sequence would exactly retrace the evolution of the first half, and no dipolar dephasing would occur. This represents a reference experiment, accounting for T_2 relaxation. REAPDOR has been used, for example, to determine ^{13}C - ^{17}O and ^{13}C - ^{14}N distances [28, 32, 33].

For homonuclear dipolar couplings between two quadrupolar nuclei different techniques have been demonstrated, which will be discussed in the next section.

Correlation Spectroscopy

In NMR of spin 1/2 nuclei correlation spectroscopy has been extremely useful in the assignment and interpretation of spectra. Spatial proximity can easily be probed, as well as bonding through hetero- and homonuclear scalar couplings in both the liquid and the solid states [1–3, 7–9, 34]. For quadrupolar nuclei similar solid-state NMR approaches have been close to nonexistent until recently. This section reviews some of the recent developments in this field.

High-Resolution Techniques

Techniques for achieving high-resolution spectroscopy of quadrupolar nuclei have been known for a long time. This was originally achieved by rotating the sample simultaneously around two axes (double rotation – DOR [35]), which removes both the first and the second order quadrupolar coupling. Another approach, which is less demanding on hardware is to rotate the sample around different axes [36] (dynamic angle spinning – DAS). As a result one obtains anisotropic–isotropic correlation spectra. The isotropic dimension shows resonances free from quadrupolar broadening effects. While these experiments have enormous potential, the practical implementations are often cumbersome due to the mechanical limitations of rapidly spinning around two different axes. In 1995 a method was developed, called multiple quantum magic angle spinning (MQMAS), which allows one to use standard hardware to obtain anisotropic–isotropic correlation spectra [37, 38]. These two-dimensional experiments show an isotropic dimension with resonances free from the first and second order quadrupolar broadenings, correlated with second order anisotropic lines in a second dimension. J couplings can therefore be resolved in this way. In particular the $J = 85 \pm 5$ Hz coupling constant between ^{11}B and ^{31}P in $(\text{PhO})_3\text{P}-\text{BH}_3$ has been determined and was used to unravel the components from the J doublet in the powder spectrum of Fig. 1 [24].

It has since been shown that the narrow resonances in the isotropic dimension show another fine structure that is related to hetero- and homonuclear through-space (dipolar) couplings [24, 39–42]. This shows up in both a linebroadening and a linesplitting. In the case of the dipolar coupling (and the anisotropic J coupling)

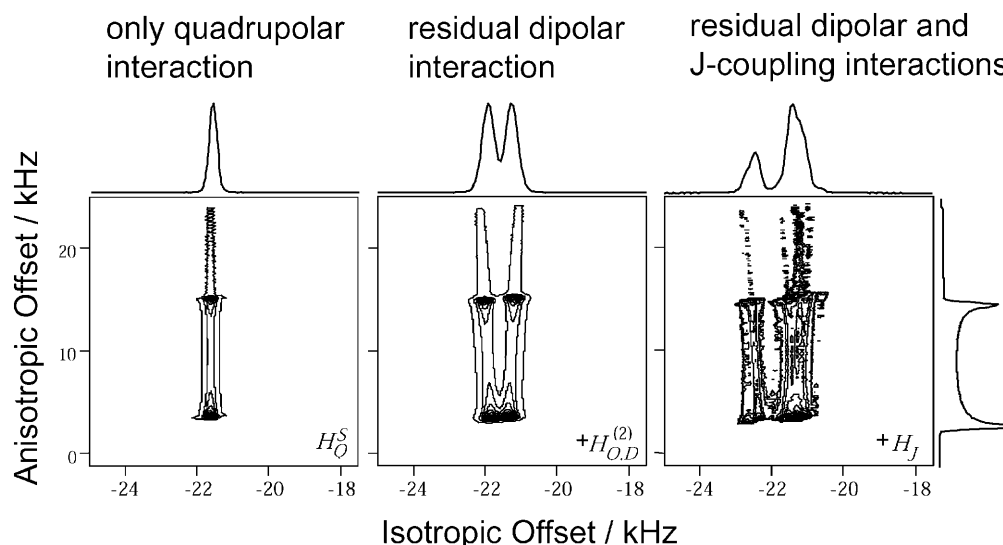


Fig. 8. Simulated 2D MQMAS NMR spectra with the quadrupolar interaction alone (a), the addition of the second order dipolar coupling (b), and the scalar coupling (c). The spectra were calculated for a pair of equivalent ^{11}B nuclear spins ($I = 3/2$) with 1.5 \AA distance in a field of 4.7 T with a quadrupolar coupling constant $C_Q = 5 \text{ MHz}$, a J coupling constant of 100 Hz, and a natural line width of 20 Hz (reproduced from Ref. [40], with permission). It should be noted that in this representation the isotropic dimension (narrow resonances) is along the horizontal axis, while the anisotropic dimension (broad resonances) is along the vertical axis. Many authors use the opposite representation

this can be explained by the same second order effect as discussed in Section 2.2. The isotropic J coupling produces a first order effect since it is not removed by MAS. For this reason, the second order dipolar coupling ($\omega_D \omega_Q / \omega_0$) is of the same order of magnitude as the J coupling (up to a few hundred Hz). Figure 8 shows an example of the fine structure observed in MQMAS spectra with both dipolar and scalar couplings present. One can therefore extract dipolar and scalar coupling parameters *via* iterative fitting to the experimental data. This process should be more accurate than fitting one-dimensional spectra, because the resonance broadening effects are not hidden by the large quadrupolar coupling.

Recently, a new type of MQMAS experiment has been presented, which produces high-resolution NMR spectra of quadrupolar nuclei by combining two different multiple quantum coherences [43]. By using different combinations of multiple quantum coherences in the experiments, one obtains different chemical shift (and quadrupolar isotropic shift) scaling factors. While heteronuclear interactions scale in exactly the same way as the chemical shift, homonuclear interactions scale differently. It is therefore expected, that combining different multiple quantum coherences for a given spin can help to increase the accuracy of iterative fits.

MQMAS spectra also display spinning sidebands in the isotropic dimension. Extraction of dipolar coupling parameters, however, appears to be difficult, since the major contribution to the sideband intensities comes from the first order quadrupolar coupling in combination with the creation and conversion efficiencies of multiple quantum coherences [44].

MQMAS has been combined with REDOR, where the dipolar dephasing sequence was applied during the multiple-quantum evolution [45]. The authors found that the sensitivity of this method for the determination of dipolar couplings is higher than for a sequence where the dipolar dephasing occurs during single quantum evolution. This is due to the fact that the heteronuclear dipolar coupling affects p quantum coherence p times stronger than single quantum coherence, hence the dephasing effect is stronger. This experiment may be a good alternative to REAPDOR and TRAPDOR in cases where efficient inversion of the multiple quantum coherence is possible.

Other, potentially more advanced methods for generating high-resolution spectra for quadrupolar nuclei have been proposed, involving the correlation of satellite transitions with central transitions [46–48]. While the peaks are broadened significantly in the isotropic dimension by inaccuracies in the setting of the magic angle, a new type of split- t_1 experiment proposed by *Wimperis* and coworkers may represent the ultimate solution to this problem [49]. It is expected that dipolar and scalar coupling interactions will be well perceptible in these experiments.

Cross-Polarization, Heteronuclear Correlation

In spin 1/2 NMR, a technique called cross-polarization (CP) is widely used to transfer magnetization from one nuclear species (usually the abundant nuclei, such as ^1H) to another (usually the rare spin, such as ^{13}C) [50–52] *via* the dipolar or the scalar couplings between those nuclei. The magnetization transfer is facilitated by the fact that the nutation frequencies of both spins are made equal by properly adjusting the respective radiofrequency fields such that $\omega_{1I} \approx \omega_{1S}$ (this is the so-called *Hartmann-Hahn* match condition [53]).

In the presence of the quadrupolar interactions the above considerations cannot be used directly to perform an efficient polarization transfer, since for many crystallites in a powder sample one has $\omega_Q \gg \omega_1$ (ω_1 is the radiofrequency field strength). The matching condition can be calculated directly in this limit [54, 55] as

$$\omega_{1I} = (S + 1/2)\omega_{1S}. \quad (1)$$

Under this condition the polarization is transferred from the I nucleus to the S (the quadrupolar) nucleus [54]. This technique can be combined with MQMAS [56, 57]. One can also transfer the polarization directly to multiple quantum coherences by using slightly modified matching conditions [55]. These experiments have also been combined with MQMAS and up to seven quantum coherence has been obtained using CP [58–62]. In the general case the sample contains also crystallites with $\omega_1 \approx \omega_Q$, so that there is no longer a clear distinction between the different matching conditions, and a suitable phase cycle needs to be used to select the proper coherence order [63].

Contrary to the situation in spin 1/2 NMR, CP in quadrupolar NMR does not in general offer signal enhancement but is more appropriately used for correlation spectroscopy and for spectral editing techniques, *i.e.* filtering out signals from nuclei that are close to spin 1/2 nuclei. Figure 9 shows an example of a correlation spectrum that can be obtained using a combination of CP and MQMAS.

Couplings in Solid State NMR

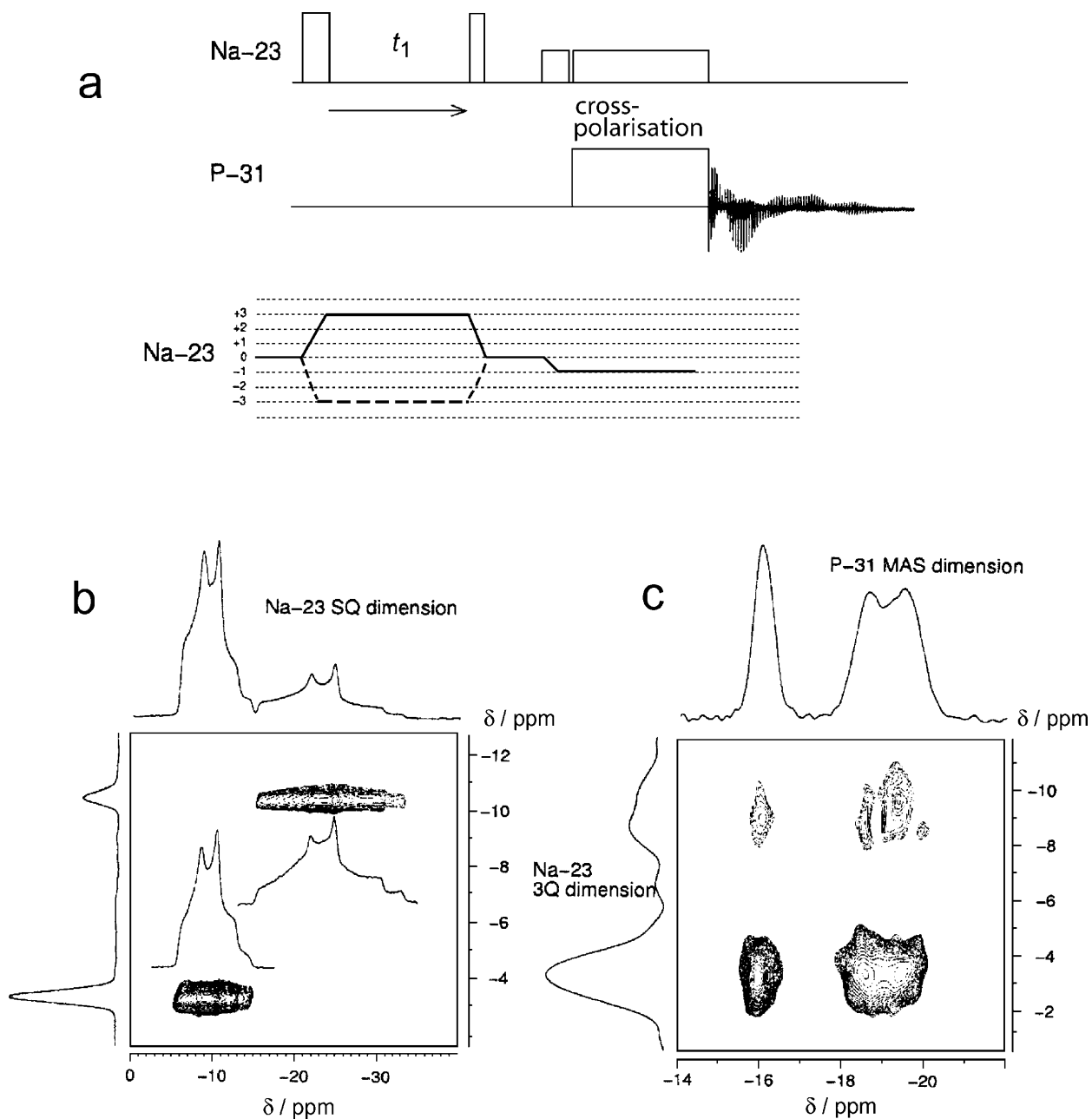


Fig. 9. (a) Pulse sequence used for the high-resolution MQMAS-CP experiment correlating the isotropic frequencies of the quadrupolar nucleus (S) with the frequencies of a spin 1/2 nucleus *via* CP. (b) The ^{23}Na 3QMAS spectrum correlating isotropic and anisotropic ^{23}Na frequencies and (c) the result of a ^{31}P - ^{23}Na correlation experiment on the compound $\text{Na}_3\text{P}_3\text{O}_9$ (reproduced from Ref. [66], with permission)

Some signal enhancement may be obtained by using “reverse” CP to transfer the polarization from the quadrupolar nucleus to spin 1/2 nucleus [64–66]. In combination with MQMAS one can obtain two-dimensional correlation experiments with

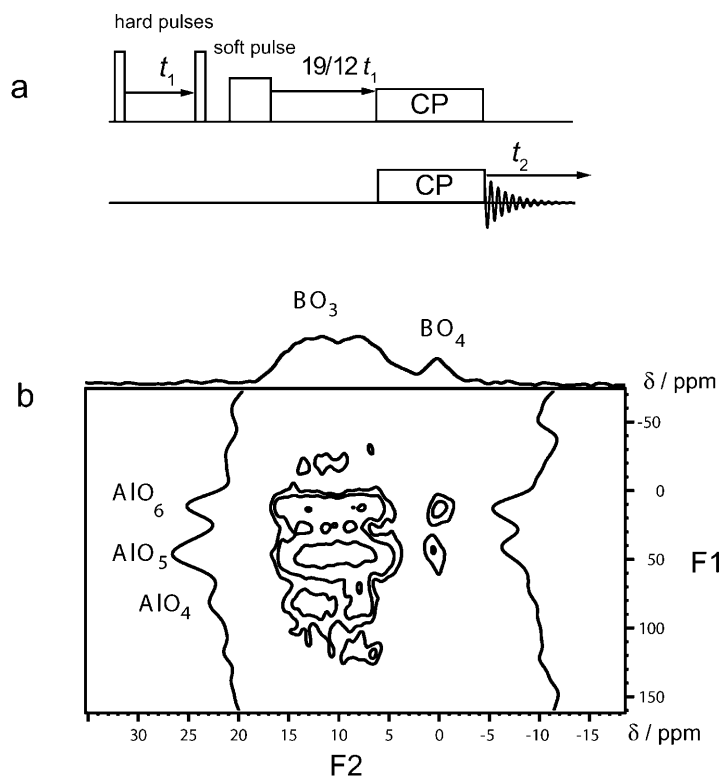


Fig. 10. (b) 2D correlation experiment between the isotropic frequencies of ^{27}Al and the anisotropic frequencies of ^{11}B . The pulse sequence for this experiment is shown in (a) (similar to the one in Fig. 9a; reproduced from Ref. [69], with permission)

an isotropic frequency dimension for the quadrupolar nucleus and a chemical shift dimension for the spin $1/2$ nucleus. Figure 9c shows a high-resolution ^{23}Na - ^{31}P correlation spectrum obtained from a sample of $\text{Na}_3\text{P}_3\text{O}_9$ [66].

The matching conditions for CP between two different quadrupolar nuclei (in this case half-integer nuclei) are yet different [67–69], and a heteronuclear correlation experiment between ^{11}B and ^{27}Al has been presented (shown in Fig. 10).

Homonuclear Recoupling

In addition to the heteronuclear dipolar interactions, the homonuclear dipolar interactions can be recoupled for the purpose of measuring distances and performing correlation experiments. By applying a properly tuned continuous wave radiofrequency field or a multiple pulse sequence it is possible to interrupt the averaging of the dipolar interactions that happens due to MAS and to recouple parts of the dipolar coupling Hamiltonian. In the quadrupolar case this technique has to be used with caution, since the same pulse sequence that recouples the homonuclear coupling will also recouple the quadrupolar coupling. Since the latter is much stronger it would lead to a quick decay of the magnetization leaving little hope that the recoupled dipolar coupling would show a perceptible effect. *Griffin* and coworkers [70] have shown that if a continuous wave field is applied which is

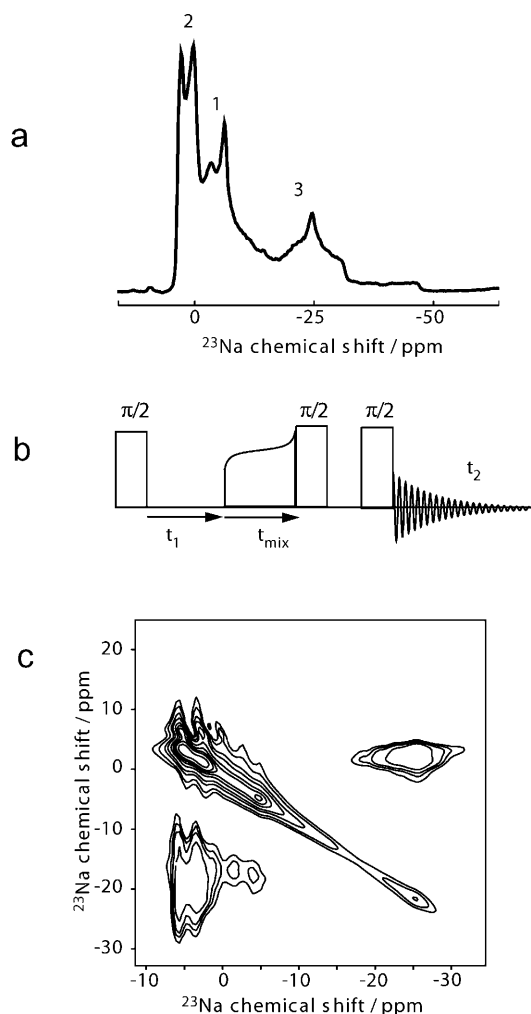


Fig. 11. (a) A one-dimensional MAS ^{23}Na spectrum indicating the three crystallographically different sites. (b) Pulse sequence and (c) spectrum for a homonuclear correlation experiment between the three crystallographically distinct ^{23}Na sites in Na_2HPO_4 (reproduced from Ref. [70], with permission)

sufficiently weak compared to the spinning speed one can keep the magnetization of the central transition locked (*i.e.* the effect of the quadrupolar coupling is minimized), while the dipolar coupling is recoupled sufficiently so that a transfer of the magnetization occurs. This has been used for a homonuclear correlation experiment between the three crystallographically distinct ^{23}Na nuclei in Na_2HPO_4 , which is shown in Fig. 11.

Meier and coworkers further showed that the magnetization can be transferred using a technique commonly known as rotational-resonance [71], and a correlation spectrum has been obtained in this way [72]. The rotational-resonance condition is met when the difference between the resonance frequencies of the two nuclei matches an integer multiple of the spinning speed. In this case the magnetization may be exchanged between the two spins. Furthermore, the authors showed that an

increase in polarization transfer can be obtained when the rotor speed is swept through the rotational-resonance condition, as in this case the matching condition is broader. This transfer has also been shown to be possible for deuterium [73].

For quadrupolar spin systems it has been shown that many more rotational resonance matching conditions can be found if a weak radiofrequency field is applied [74–76]. These effects can be exploited for enhancing the excitation efficiency in MQMAS experiments on the one hand, but more importantly can be used to create three-dimensional high-resolution correlation experiments based on homonuclear dipolar couplings [77].

For completeness, we also mention that by offsetting the sample spinning axis from the magic angle, one also reintroduces the dipolar couplings, which has been used to obtain a correlation spectrum for a ^{23}Na and ^{11}B -containing sample [78].

Other Methods

As a final note we would like to mention a curious correlation experiment that was recently presented by *Duer and Painter* [79]. In this experiment dipolar coupling between two $3/2$ quadrupolar nuclei (^{23}Na) is probed by creating six quantum coherence between them. This high quantum coherence can only be created when two of these spins are in close proximity. Formally, this experiment corresponds to the INADEQUATE experiment for spin $1/2$ nuclei, where double quantum coherence is created between the two nuclei [80].

Conclusions

In this article an overview was presented over manifestations of dipolar and scalar couplings in quadrupolar NMR. We mentioned linebroadening and linesplitting effects in one-dimensional NMR, methods for recoupling of the dipolar interaction in MAS spectra, residual couplings in high-resolution MQMAS experiments, and some of the more recent hetero- and homonuclear correlation experiments. The development of high-resolution methods has unveiled the underlying structure of the NMR interactions, which are normally completely hidden by the quadrupolar interactions. The focus on dipolar and scalar coupling interactions is a natural development in this area, as it is through these couplings that some of the most sophisticated NMR experiments provide structural information both in liquid and in solid state NMR today. It is probably only a matter of time until powerful hetero- and homonuclear solid-state correlation experiments of quadrupolar nuclei will become routine techniques.

References

- [1] Cavanagh J, Palmer AG, Fairbrother W, Skelton N (1996) *Protein Nmr Spectroscopy: Principles and Practice*. Academic Press, San Diego
- [2] Davis J, Auger M (1999) *Prog Nucl Magn Reson Spectroscopy* **35**: 1
- [3] Wüthrich K (1996) *The Encyclopedia of NMR*, vol 2, Wiley, NY, pp 932–939
- [4] Dusold S, Sebald A (2000) *Annu Rep NMR Spectrosc* **41**: 185
- [5] Bennett AE, Griffin RG, Vega S (1994) *NMR Bas Princ Progr* **33**: 3

Couplings in Solid State NMR

- [6] Gullion T, Schaefer J (1989) *J Magn Reson* **81**: 196
- [7] Rienstra CM, Hohwy M, Hong M, Griffin RG (1998) *J Am Chem Soc* **120**: 10602
- [8] Fyfe CA, Grondey H, Feng Y, Kokotailo GT (1990) *Chem Phys Lett* **173**: 211
- [9] Lesage A, Charmont P, Steuernagel S, Emsley L (2000) *J Am Chem Soc* **122**: 9739
- [10] Hardy EH, Verel R, Meier BH (2001) *J Magn Reson* **148**: 459
- [11] Heindrichs ASD, Geen H, Giordani C, Titman JJ (2001) *Chem Phys Lett* **335**: 89
- [12] Laws DD, Bitter HML, Jerschow A (2002) *Angew Chem Int Ed Engl* (in press)
- [13] Vega AJ (1996) *The Encyclopedia of NMR*, vol 4, Wiley, NY, pp 3869–3888
- [14] Herzfeld J, Berger AE (1980) *J Chem Phys* **73**: 6021
- [15] Davies NA, Harris RK, Olivieri AC (1996) *Mol Phys* **87**: 669
- [16] Olivieri AC (1997) *Solid State Nucl Magn Reson* **10**: 19
- [17] Ding S, McDowell A (1997) *J Chem Phys* **107**: 7762
- [18] Wu G, Kroeker S, Wasylshen RE, Griffin RG (1997) *J Magn Reson* **124**: 237
- [19] Asaro F, Camus A, Gobetto R, Olivieri AC, Pellizer G (1997) *Solid State Nucl Magn Reson* **8**: 81
- [20] Hexem JG, Frey MH, Opella SJ (1982) *J Chem Phys* **77**: 3847
- [21] Harris RK, Olivieri AC (1992) *Prog NMR Spectrosc* **24**: 435
- [22] Jonsen P, Olivieri AC, Tanner SF (1996) *Solid State Nucl Magn Reson* **7**: 121
- [23] Wi S, Frydman L (2000) *J Chem Phys* **112**: 3248
- [24] Wu G, Yamada K (1999) *Chem Phys Lett* **313**: 519
- [25] Chan JCC, Bertmer M, Eckert H (1999) *J Am Chem Soc* **121**: 5238
- [26] Bertmer M, Züchner L, Chan JCC, Eckert H (2000) *J Phys Chem B* **104**: 6541
- [27] van Eck ERH, Kentgens APM, Kraus H, Prins R (1995) *J Phys Chem* **99**: 16080
- [28] Smith ME, van Eck ERH (1999) *Progr Nucl Magn Reson Spectrosc* **34**: 159
- [29] van Wüllen L, Kalwei M (1999) *J Magn Reson* **139**: 250
- [30] Kao H, Grey CP (1996) *Chem Phys Lett* **259**: 459
- [31] Deng F, Yue Y, Ye C (1998) *Solid State Nucl Magn Reson* **10**: 151
- [32] Gullion T (1995) *Chem Phys Lett* **246**: 325
- [33] Gullion T (1995) *J Magn Reson Series A* **117**: 326
- [34] Pauli J, van Rossum B, Förster H, de Groot HJM, Oschkinat H (2000) *J Magn Reson* **143**: 411
- [35] Samoson A, Lippmaa E, Pines A (1988) *Mol Phys* **65**: 1013
- [36] Llor A, Virlet J (1988) *Chem Phys Lett* **152**: 248
- [37] Frydman L, Harwood J (1995) *J Am Chem Soc* **117**: 5367
- [38] Medek A, Harwood JS, Frydman L (1995) *J Am Chem Soc* **117**: 12779
- [39] McManus J, Kemp-Harper R, Wimperis S (1999) *Chem Phys Lett* **311**: 292
- [40] Wi S, Frydman L (2000) *J Chem Phys* **112**: 3248
- [41] Wi S, Frydman V, Frydman L (2001) *J Chem Phys* **114**: 8511
- [42] Pike KJ, Malde RP, Ashbrook SE, McManus J, Wimperis S (2000) *Solid State Nucl Magn Reson* **16**: 203
- [43] Jerschow A, Logan JW, Pines A (2001) *J Magn Reson* **149**: 268
- [44] Marinelli L, Frydman L (1997) *Chem Phys Lett* **275**: 188
- [45] Pruski M, Bailly A, Lang DP, Amoureux JP, Fernandez C (1999) *Chem Phys Lett* **307**: 35
- [46] Gan Z (2000) *J Am Chem Soc* **122**: 3242
- [47] Pike KJ, Ashbrook SE, Wimperis S (2001) *Chem Phys Lett* **345**: 400
- [48] Ashbrook SE, Wimperis SJ (2002) *J Magn Reson* **156**: 269
- [49] Ashbrook SE, Wimperis S (2002) *ENC Conference Asilomar California*, Poster M/T73
- [50] Pines A, Gibby MG, Waugh JS (1973) *J Chem Phys* **59**: 569
- [51] Stejskal EO, Schaefer J, Waugh JS (1977) *J Magn Reson* **28**: 105
- [52] Schaefer J, Stejskal EO (1976) *J Am Chem Soc* **98**: 1031
- [53] Hartmann SR, Hahn EL (1962) *Phys Rev* **128**: 2042
- [54] Vega AJ (1992) *Solid State Nucl Magn Reson* **1**: 17

- [55] Vega S (1981) *Phys Rev A* **23**: 3152
- [56] Ashbrook SE, Wimperis S (2001) *Chem Phys Lett* **340**: 500
- [57] Fernandez C, Delevoye L, Amoureux JP, Lang DP, Pruski M (1997) *J Am Chem Soc* **119**: 6858
- [58] Ashbrook SE, Wimperis S (2000) *Mol Phys* **98**: 1
- [59] Ashbrook SE, Brown SP, Wimperis S (1998) *Chem Phys Lett* **288**: 509
- [60] Rovnyak D, Baldus M, Griffin RG (2000) *J Magn Reson* **142**: 145
- [61] Lim KH, Grey CP (2000) *J Chem Phys* **112**: 7490
- [62] Lim KH, Grey CP (1999) *Chem Phys Lett* **312**: 45
- [63] Ashbrook SE, Wimperis S (2000) *J Magn Reson* **147**: 238
- [64] De Paul SM, Ernst M, Shore JS, Stebbins JF, Pines A (1997) *J Phys Chem B* **101**: 3240
- [65] Wang SH, De Paul SM, Bull LM (1997) *J Magn Reson* **125**: 364
- [66] Steuernagel S (1998) *Solid State Nucl Magn Reson* **11**: 197
- [67] Eastman MA (1999) *J Magn Reson* **139**: 98
- [68] Chan JCC, Bertmer M, Eckert H (1998) *Chem Phys Lett* **292**: 154
- [69] Chan JCC (1999) *J Magn Reson* **140**: 487
- [70] Baldus M, Rovnyak D, Griffin RG (2000) *J Chem Phys* **112**: 5902
- [71] Raleigh DP, Levitt MH, Griffin RG (1988) *Chem Phys Lett* **146**: 71
- [72] Nijman M, Ernst M, Kentgens APM, Meier BH (2000) *Mol Phys* **98**: 161
- [73] Gan Z, Robyr P (1998) *Mol Phys* **95**: 1143
- [74] Walls J, Lim K, Pines A (2002) *J Chem Phys* **116**: 79
- [75] Walls JD, Lim KH, Logan JW, Urban JT, Jerschow A, Pines A (2002) *J Chem Phys* **117**: 518
- [76] Logan JW, Urban JT, Walls JD, Lim KH, Jerschow A, Pines A (2002) *Solid State Nucl Magn Reson* (in press)
- [77] Wi S, Heise H, Logan J, Sakellariou D, Pines A (2002) ENC Conference Asilomar California, Poster W/Th66
- [78] Hartmann P, Jäger C, Zwanziger JW (1999) *Solid State Nucl Magn Reson* **13**: 245
- [79] Duer MJ, Painter AJ (1999) *Chem Phys Lett* **313**: 763
- [80] Bax A, Freeman R, Frenkiel TA (1981) *J Am Chem Soc* **103**: 2102
- [81] Wu G, Dong S (2001) *Chem Phys Lett* **334**: 265